



Trade Science Inc.

# Research & Reviews In Polymer

---

*Full Paper*

RRPL, 2(2), 2011 [57-64]

## Preparation of polymer composite by using hydrothermally synthesized titanium oxide fillers and its characterization

H.P.Shivaraju

Guest Faculty for Environmental Science, Department of Environmental Science,  
Yuvaraja Collage, University of Mysore, Mysore 570 006, (INDIA)

E-mail: shivarajuenvi@gmail.com

Received: 14<sup>th</sup> June, 2011 ; Accepted: 14<sup>th</sup> July, 2011

### ABSTRACT

Metal-oxide nanoparticles can be used to optimize UV absorption and to enhance the stiffness, toughness, and probably the service life of polymeric materials. In the present study TiO<sub>2</sub> nanoparticles were synthesized under mild hydrothermal conditions (Temperature > 200 °C and Experimental duration >24 h) and as prepared TiO<sub>2</sub> nanoparticles are inserted into polyurethane (PU) matrix. Polymer-TiO<sub>2</sub> composites have been prepared using castor oil based polyurethane as a host and TiO<sub>2</sub> as particulate filler. The prepared PU/TiO<sub>2</sub> composites have been characterized for mechanical properties such as tensile strength and tensile modulus. These PU composites exhibited an improved mechanical performance compared to the unfilled PU. PU/TiO<sub>2</sub> composites were prepared by varying amounts of TiO<sub>2</sub> fillers (2.5%, 5%, and 10%) in PU matrix. As obtained PU/TiO<sub>2</sub> composites were characterized by analytical techniques like XRD, FTIR, SEM to study the nanostructure and dispersion of TiO<sub>2</sub> nanoparticles in PU matrix and structure-property relationships. Microstructure, chemical elucidation, TiO<sub>2</sub> particles dispersed and other characterizations of PU/TiO<sub>2</sub> composites obtained are discussed. The photocatalytic activity and weight loss under the aqueous medium was investigated and mechanistic aspects of the liquid-phase photocatalytic activity, and photodecomposition, their implication for developing photo decomposable polymer composites were discussed. © 2011 Trade Science Inc. - INDIA

### KEYWORDS

Nanoparticle;  
Hydrothermal conditions;  
Polyurethane;  
Castrol oil;  
Mechanical properties;  
Tensile strength.

### INTRODUCTION

Nowadays the enormous use of polymer materials is attributed to their extraordinary combination of properties, low weight and ease of processing. However for improvement of some properties such as thermal and mechanical stability, large numbers of additives were added to polymeric matrix and formed polymer matrix

composite<sup>[1,2]</sup>. To improve the properties of composite materials investigate composites with lower and lower fillers size, leading to the development of microcomposites and the recent trend in composite research is nanocomposites. Nanocomposites refer to composites in which one phase has nanoscale morphology such as nanoparticles, nanotubes or lamellar nanostructure<sup>[1-4]</sup>. The improvement of the properties

## Full Paper

by the addition of particles can be achieved when adequately good interaction between the nanoparticles and the matrix and good dispersion of particles within the matrix. In nanocomposites, covalent bonds, ionic bonds, Vander Waals forces, hydrogen bonding could exist between the matrix and filler components<sup>[3]</sup>. The use of renewable resources has attracted the attention of many researchers due to their application potential as substitutes for petrochemical derivatives. Much attention has been focused on the innovation and development of newer materials from renewable resources, i.e., forest products that could be grown again and again. One of the most naturally and abundantly occurring vegetable oil is castor oil. Castor oil possesses both unsaturated and conjugated hydroxyl functional groups. Castor oil reacts with different diisocyanates, which is also polyfunctional to form polyurethane (PU)<sup>[5-7]</sup>. Chain extended PU elastomers have a wide range of industrial applications and they are well known for their mechanical properties. These polymers typically exhibit a two-phase morphology because of the incompatibility of hard and soft segments. The excellent mechanical properties of polyurethane such as high tensile strength and toughness are primarily a result of the two-phase microstructure from this phase separation<sup>[8,9]</sup>. Metal-oxide particles such as TiO<sub>2</sub> and ZnO, serve many functions in the various polymeric materials. Traditionally, they have been used as pigments to enhance the appearance and improve the durability of polymeric products, and usually they have been considered to be inert. As nanosized particles, these materials exhibit broad band UV absorption, a benefit that currently has been exploited only in sunscreen applications. Also, the addition of nanoparticles would likely enhance the stiffness, toughness, and service life of polymeric materials, for example, in applications in which mar resistance is important. Optimizing the material properties of metal-oxide nanoparticle/polymer composites, the microstructure and dispersion (sizes and spatial distribution) of nanoparticles must be characterized as a function of different process conditions. Composite materials have a wonderful and different range of applications. Important advantages of composites over many metal compounds are high specific stiffness and specific strength, high toughness, corrosion resistance, low density and thermal insulation<sup>[1,2]</sup>. It is interesting to note that the

solid-phase photocatalytic degradation of polymer-TiO<sub>2</sub> composites has been known and studied for quite a long time in relation to the *chalking* phenomenon in the pigmented paint/polymer systems<sup>[10]</sup>. Several studies on photodegradation of TiO<sub>2</sub>-blended polymer in air such as polyethylene<sup>[11]</sup> and PVC<sup>[12,13]</sup> have been carried out. However, their main interests focused on inhibiting the photocatalytic activity of TiO<sub>2</sub> in relation to weathering of the polymer composites. The present study tried to take advantage of such effects on the contrary. Unlike their liquid - or gas-phase counterpart, the solid -phase photocatalytic reactions have been far less studied and little is known for their mechanistic pathways. It needs to be understood how they initiate and propagate within the solid matrix for the development of efficient photo-degradable polymer composites. Whereas the number of metal oxides is small and limited, that of organic and biological molecules is vast and virtually unlimited. Naturally, hybridization of these two parent families can enrich the property library and widen the application scope offered by each of them individually. Recently, this principle has been behind a series of studies<sup>[14-19]</sup> that introduced a new family of materials, designated as organic compound-doped by metal oxides. The unique properties of titanium oxide (TiO<sub>2</sub>) make them one of the most useful inorganic materials in the world. Polymers constitute very important host materials for a variety of filler materials leading to the formation of composites with technological potential. In recent years, there is a growing tendency to search for new properties for materials like TiO<sub>2</sub>, AlPO<sub>4</sub> and ZnO filled polymer composites, optically active molecules such as non-linear optical materials, luminescent materials, catalytic materials, etc. Hence, we have selected PU as the matrix with TiO<sub>2</sub> as the particulate filler in order to establish structure-property relationship. The present work deals with the influence of TiO<sub>2</sub> particulate filler on the performance of the PU composites.

## MATERIALS AND METHODOLOGY

Castor oil was obtained from the local market and it was dried over night at 90 °C before use. Its average molecular weight (Mn) is 930, and hydroxyl group per molecule is 2.24. Toluene diisocyanate (TDI), dibutyl tin dilaurate (DBTL) (catalyst) and tartaric acid (TA)

supplied by Fluka were used without dilution and distillation. Methyl ethyl ketone (MEK) of AR grade was used after distillation. Other chemicals such as  $\text{TiO}_2$ , orthophosphoric acid and di-propylamine of AR grade were procured from Aldrich, USA.

### Preparation of $\text{TiO}_2$ filler

$\text{TiO}_2$  nanoparticles were synthesized under mild hydrothermal conditions ( $T=150^\circ\text{C}$ ,  $P$ = autogeneous). 1M of pure  $\text{TiO}_2$  was taken as starting material and a known amount of 1M HCl was added as mineralizer to the precursors. The mixture was stirred vigorously for a few minutes. The final compound was then transferred to the Teflon liner ( $V_{\text{fill}}=10\text{ mL}$ ), which was later placed inside a General-Purpose autoclave. Then the assembled autoclave was kept in an oven with a temperature programmer-controller for 24 h. The temperature was kept at  $150^\circ\text{C}$ . After the experimental run, the autoclave was cooled to the room temperature. The product in Teflon liner was then transferred to a clean beaker, washed with double-distilled water, and later allowed the product to settle down. The surplus solution was removed using a syringe and the remnants were centrifuged for 20 minutes at 1500 rpm. The product was recovered and dried in a hot air oven at  $40\text{--}50^\circ\text{C}$  for a few hours. As obtained  $\text{TiO}_2$  nanoparticles were fabricated and stored in desiccators. Further this material was used as filler in polyurethane matrix.

### Preparation of PU/ $\text{TiO}_2$ polymer composite

Castor oil (0.001 M) was initially dissolved in 50 ml of MEK and placed in three-necked round bottomed flask. Toluene diisocyanate (0.002 M) was added followed by two to three drops of DBTL as catalyst and the contents of the flask were stirred continuously for about 1 h under oxygen free nitrogen gas purge at  $60\text{--}70^\circ\text{C}$ , to prepare the isocyanate-terminated pre PU polymer. Calculated amount of tartaric acid (0.001 M) weighed accurately, was completely dissolved in 10 ml MEK and added to the pre PU and stirred for 1 h, under nitrogen gas purge at  $65\text{--}70^\circ\text{C}$ . The calculated amount of  $\text{TiO}_2$  filler was added at this stage and stirred for 10 to 20 min or until the uniform mixture was obtained. The solution was degassed under vacuum, and poured into cleaned glass mould and allowed for 12 h at room temperature. The mould was kept in preheated circulating

hot air oven at  $70^\circ\text{C}$  for 8–10 h. The toughened PU composite sheet thus formed was cooled slowly and removed from the mould. The above procedure was repeated for different  $\text{TiO}_2$  filler contents, viz. 2.5, 5 and 10 by weight percent. A flow chart of preparation of PU/ $\text{TiO}_2$  composite is shown in Figure 1.

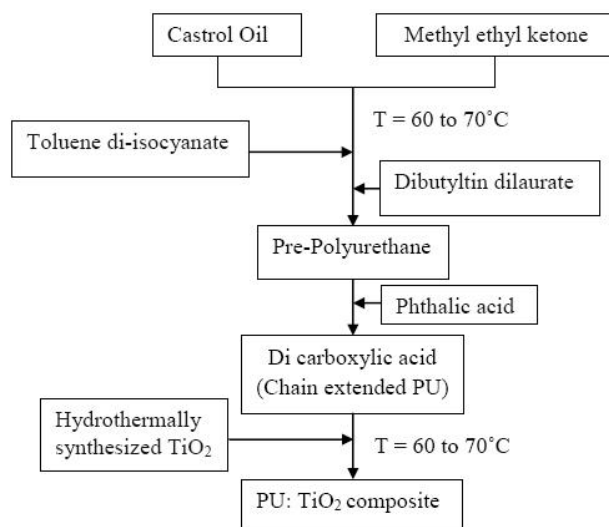


Figure 1 : Flow chart showing the preparation of PU/ $\text{TiO}_2$  composite

### Characterization methods

The prepared tartaric acid chain extended PU and its composites were characterized for surface hardness according to ASTM D 785 method. Mechanical properties such as tensile strength and tensile modulus have been performed as per ASTM D 638 method using 4302 model Hounsfield universal testing machine (UTM), UK. Minimum six samples were tested at room temperature for each formulation and the average values are reported. The XRD studies were also carried out using the RIGAKU, Ultima III Series, TSX System, Japan at a scanning speed of  $2^\circ/\text{min}$ , and  $2\theta$  ranging from 70 to 10 degrees with Cu target emitting the  $\text{Cu K}\alpha$  radiations with the operating current and voltage of 15 mA and 30 kV respectively. The identification of the crystalline phases was carried out by comparison with Joint Committee on Powder Diffraction Standards (JCPDS) database using PCPDF Win version 2.01<sup>[20,21]</sup>. The structural and quantitative elucidation of PU/ $\text{TiO}_2$  composites were characterized by the Fourier Transform Infrared Spectroscopy (JASCO-460 PLUS, Japan) in the range of  $400\text{--}4000\text{ cm}^{-1}$  at resolution of  $4\text{ cm}^{-1}$ . The sample holder of the instru-

## Full Paper

ment has a provision for the measurement of blank KBr as well as for the sample. The sample is prepared by mixing thoroughly with KBr and compound whose FTIR to be recorded in the ratio of 100:3. The background measurements were recorded for blank KBr before measuring the sample. The programme of the instrument has provision for automatic correction for background in the sample measurements. The spectrum obtained has been analyzed using JASCO Spectra analysis programme and JASCO file find programme. The surface morphology of PU composites was studied using a scanning electron micrograph (model HITACHI S- 4200). The micrographs of the composites were taken on SX-50 with probe microanalysis SI. 320 after gold (100Å) coating. The magnification is displayed on the respective microphotographs of the samples. Photocatalytic activity of PU/TiO<sub>2</sub> composites was carried out under UV light in aqueous medium by following standard method<sup>[22-25]</sup>. Each sample was weighed before and after irradiation to monitor the weight loss as a result of photodecomposition under different conditions.

## RESULTS AND DISCUSSION

Well crystalline TiO<sub>2</sub> nanoparticle were synthesized under mild hydrothermal conditions and used as filler for the preparation of polyurethane composite. Physical and chemical properties of as prepared composite were studied systematically. The mechanical properties are very important in selecting a polymer material for suitable applications. The PU/TiO<sub>2</sub> composites were obtained as tough films with golden yellow color. The measured mechanical properties such as surface hardness, tensile strength and modulus, % elongation at break and density of the PU/ TiO<sub>2</sub> composites are given in TABLE 1. Surface hardness data reflects the resistance to local deformation, which is a complex property, related to cross-link density, modulus, strength, elasticity, plasticity and porosity of the polymer matrix. A slight increase in surface hardness values with increase in filler content was found and which falls in the range 25 to 44 Shore D. The increase in surface hardness with increase in TiO<sub>2</sub> is due to the reinforcing behavior of filler and good physical interaction between PU and TiO<sub>2</sub> nanoparticles. The incorporation of TiO<sub>2</sub> filler in the PU

matrix seems to increase the dimensional stability with increase in filler content. A considerable improvement in both tensile strength and tensile modulus of composites with increase in filler content in PU matrix was noticed. Tensile strength and tensile modulus fall in the range 3.21–6.88 MPa and 2.96–5.71 MPa respectively (TABLE 1). The improvement in the tensile strength and tensile modulus with increase in filler content is due to good interaction and interfacial adhesion between PU and TiO<sub>2</sub> filler. Percent elongation at break and overall density of PU/TiO<sub>2</sub> composite also increased with increased wt % TiO<sub>2</sub> filler in PU matrix. A considerable increase in dimensional stability, tensile strength and drastic improvement in tensile modulus clearly supports the reinforcing behavior of TiO<sub>2</sub> fillers in PU matrix. Figure 2 showed the stress and strain curve of PU/ TiO<sub>2</sub> composites and it clearly indicating that considerable increased rate of stress and strain with respect to increased Wt % of TiO<sub>2</sub> filler in PU matrix. Mechanical properties are higher for TiO<sub>2</sub> filler reinforced PU composites compared to unreinforced PU indicating the good reinforcement by TiO<sub>2</sub> filler.

TABLE 1 : Mechanical properties of PU/ TiO<sub>2</sub> composites

PU/TiO <sub>2</sub> Composites (in Wt %)	Tensile Strength (MPa)	% Elongation at Break	Tensile Modulus (MPa)	Surface hardness (Shore D)	Density (g/cm <sup>3</sup> )
Blank PU	3.21	218	2.96	25	1.02
PU+2.5% PU	3.55	250	3.4	29	1.35
PU+5% PU	4.67	281	3.95	36	1.85
PU+10% PU	6.88	393	5.71	41	2.13
TiO <sub>2</sub> Particles					4.23

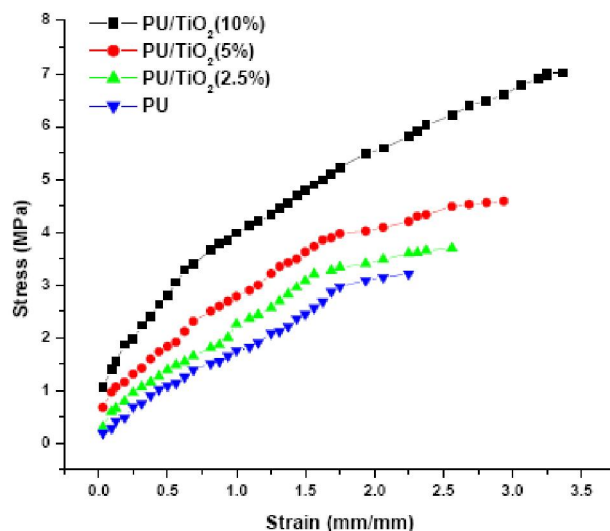


Figure 2 : Stress and strain curve of PU/ TiO<sub>2</sub> composites

The X-ray patterns of hydrothermally synthesized  $\text{TiO}_2$ , pure PU and PU/ $\text{TiO}_2$  composites are shown in Figure 3. The hydrothermally synthesized  $\text{TiO}_2$  shows stronger peaks at  $25.4^\circ$  (Figure 3a). The crystalline phase of  $\text{TiO}_2$  identified matches well with PCPDF-841285 and it confirmed as anatase phase of  $\text{TiO}_2$  obtained under hydrothermal conditions. The unfilled PU matrix showed single broad peaks at  $2\theta$  of  $20.0^\circ$ . The X-ray pattern of  $\text{TiO}_2$  filler shows multiple sharp peaks. This is due to highly crystalline nature of  $\text{TiO}_2$  filler than that of chain extended PU. After incorporation of  $\text{TiO}_2$  filler into PU matrix, the peaks shape, size and position are changed. The PU/ $\text{TiO}_2$  composite showed one sharp peaks at  $20.0^\circ$  and  $25.4^\circ$ . Also the peak position and intensity changed with composition of composites. This is due to change in microcrystalline behavior of composites with increase in filler content. The calculated crystalline cell parameters including the cell volumes of PU/ $\text{TiO}_2$  composites are given in TABLE 2. The cell parameters were calculated using the Check cell software. The cell volume is lowest for  $\text{TiO}_2$  ( $136.251.3 \text{ \AA}^3$ ) and highest for PU ( $1000.710 \text{ \AA}^3$ ). For composites, cell volume increases significantly with increase in filler content and it lies in the range of  $1110.7$ – $1806.5 \text{ \AA}^3$ . This result clearly indicates physical interaction between PU and  $\text{TiO}_2$ . The data obtained from X-ray diffraction patterns showed the physical interaction or interfacial adhesion between the PU and well crystalline  $\text{TiO}_2$  filler.

Figure 4 showed the FTIR spectra of  $\text{TiO}_2$ , PU and PU/ $\text{TiO}_2$  composite. PU/ $\text{TiO}_2$  composite and PU presented the same spectra in the wave number range of  $400$ – $4000 \text{ cm}^{-1}$  while the weak peak located at  $500$ – $700 \text{ cm}^{-1}$  is attributed to the stretching of Ti–O bond. FTIR spectra of PU and polymer composites show a narrow peaks attributed to the urethane carbonyl (C=O) stretching at  $1710 \text{ cm}^{-1}$  and stretching of the different C-H groups at  $3084$ ,  $2985$  and  $2933 \text{ cm}^{-1}$  are probably due to C-H aromatic, C-H asymmetric and symmetric vibrations. The amine groups such as C-N stretching and H-N stretching bands are found at the range  $1320 \text{ cm}^{-1}$  and  $1650 \text{ cm}^{-1}$  respectively. The broad and strong vibration stretching band of H-O group found at the range of  $2500$  to  $3500 \text{ cm}^{-1}$ . The  $\text{TiO}_2$  stretching band in the FTIR spectra of PU/ $\text{TiO}_2$  composite is observed at the range in between the  $800$  to  $500 \text{ cm}^{-1}$ .

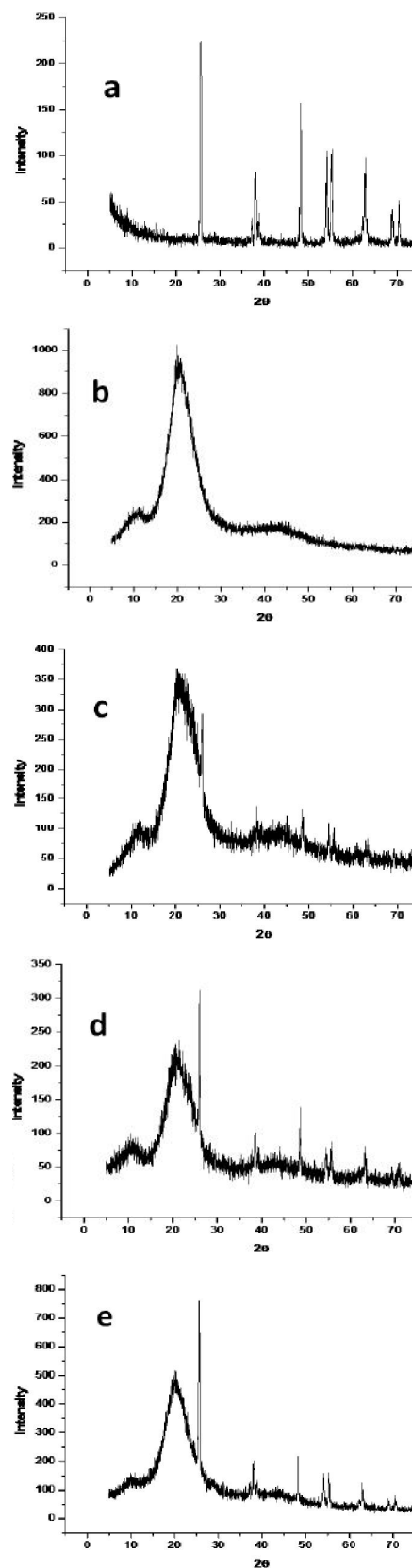
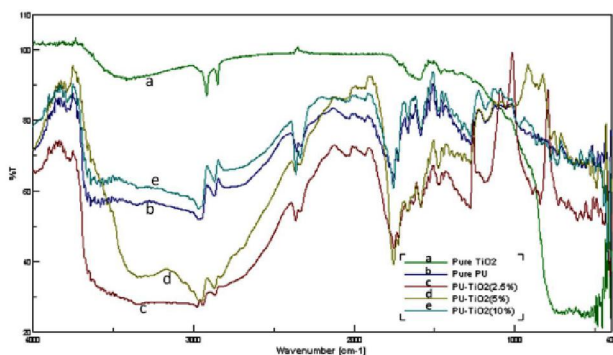


Figure 3: X-ray patterns of (a) hydrothermally synthesized  $\text{TiO}_2$ ; (b) pure PU; (c) PU/ $\text{TiO}_2$  (2.5 wt %); (d) PU/ $\text{TiO}_2$  (5 wt %); (e) PU/ $\text{TiO}_2$  (10 wt %)

## Full Paper

**TABLE 2 : Cell parameters obtained for PU/TiO<sub>2</sub> filler composite**

PU/TiO <sub>2</sub> composite (in Wt %)	Cell parameters						
	a (Å)	b (Å)	c (Å)	Alpha	Beta	Gamma	Volume (Å <sup>3</sup> )
TiO <sub>2</sub>	3.7842	3.7842	9.5146	90	90	90	136.251
Blank PU	5.9043	7.6116	25.960	95.96	115.34	71.74	1000.710
PU+2.5% PU	8.9853	10.727	12.525	90.28	109.56	78.11	1110.635
PU+5% PU	9.9104	12.017	14.213	90.07	109.79	79.91	1565.146
PU+10% PU	9.4526	12.469	16.522	90.13	109.35	80.03	1806.517



**Figure 4 : FTIR spectra of PU/ TiO<sub>2</sub> composites**

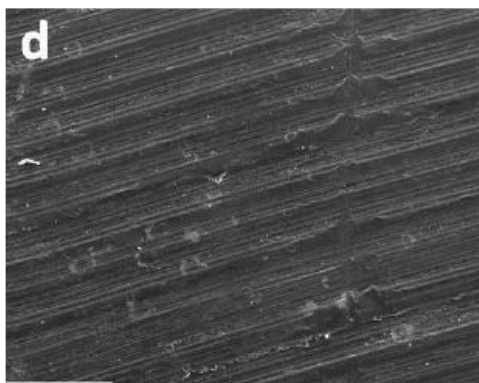
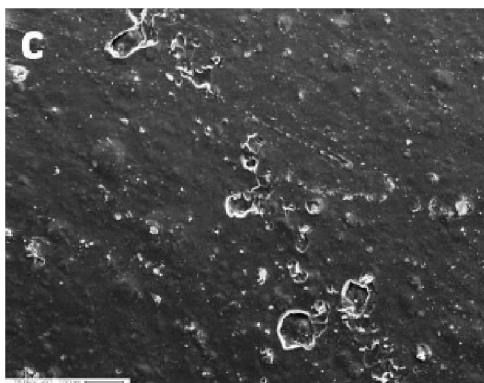
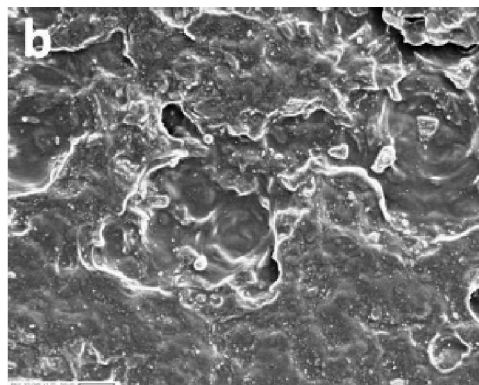


**Figure 5 : SEM images of (a) pure PU; (b) PU/TiO<sub>2</sub> (2.5 wt %); (c) PU/TiO<sub>2</sub> (5 wt %); (d) PU/TiO<sub>2</sub> (10 wt %)**

Photocatalytic experiments were carried out under UV light using 0.0001M Indigo Carmine dye solution of pH 6.8. Figure 6 showed the photocatalytic activity of pure TiO<sub>2</sub> and PU/TiO<sub>2</sub> composites. The surface hy-

This result led to the conclusion that there were no major chemical structure changes in PU owing the presence of small amount of TiO<sub>2</sub> filler.

The surface morphology of chain-extended PU composites was studied by SEM. The electron photo micrographs of the surface of the composites are shown in Figure 5. From SEM photographs, two-phase morphology for PU was noticed. This is because chain extended PUs consists of both hard and soft segments. The SEM microphotographs also reveal that distribution of TiO<sub>2</sub> filler in PU matrix as a continuous phase. The TiO<sub>2</sub> filler is embedded in the PU matrix, which may be due to physical interaction between PU and filler. As the TiO<sub>2</sub> filler content increases, the domain size of second dispersed phase also increased, which may be due to the small agglomeration of TiO<sub>2</sub> filler. In the present investigation, in all the PU/ TiO<sub>2</sub> composites uniform distribution of second phase was noticed.

Photocatalytic activity of PU/TiO<sub>2</sub> composite was studied by using standard experimental procedures<sup>[22-25]</sup>.

droxyl groups on TiO<sub>2</sub> react with valence band (VB) holes to generate hydroxyl radicals, which are responsible for most of the oxidizing power of TiO<sub>2</sub> photocatalysts. In aqueous suspensions or in contact

with water vapors in the gas-phase, the surface OH group density remains unchanged during irradiation since the depleting OH groups are continuously replenished. The results obtained showed that PU/TiO<sub>2</sub> composites performed very less photocatalytic activity when compared to pure TiO<sub>2</sub> particles. On the other hand, in the present case TiO<sub>2</sub> particles were buried in the polymer matrix. The short length propagation of light in the polyurethane matrix will reduce the enough photon energy receive for activation of buried TiO<sub>2</sub> under UV light. Less transmission of light through the PU matrix limits the photons to reach TiO<sub>2</sub> surface and it significantly decreases the photocatalytic activity of PU/TiO<sub>2</sub> composites.

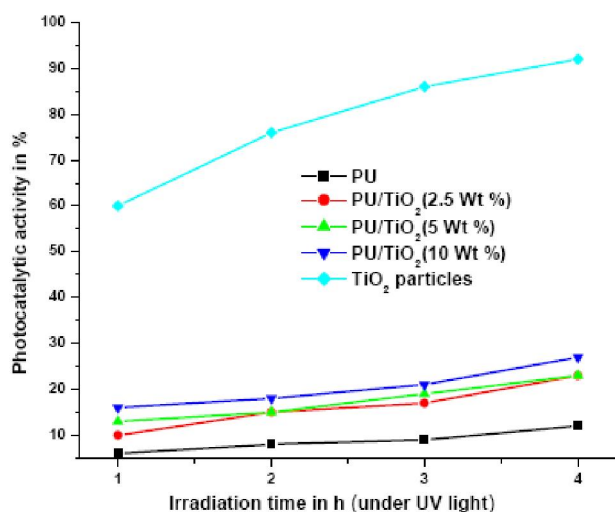


Figure 6 : Photocatalytic activities of pure TiO<sub>2</sub> and PU/ TiO<sub>2</sub> composites

Photocatalytic decomposition weight loss of PU and PU/ TiO<sub>2</sub> composites were studied under UV light in aqueous medium. Figure 7 showed the photoinduced weight loss of the PU films under aqueous medium. The weight loss rates were much higher for the PU/TiO<sub>2</sub> composites than the pure PU film. The weight loss of the PU/TiO<sub>2</sub> composites films steadily decreased with irradiation under aqueous medium and led to the total 30% (PU/TiO<sub>2</sub> 10 Wt % fill) reduction in 250 h while the PU film showed only 8 % weight loss under the identical experimental condition. The presence of O<sub>2</sub> was essential for the efficient photolytic degradation of PU. The photocatalytic decomposition of the PU matrix in the solid-phase seems to be initiated by active oxygen species (e.g. O<sup>2-</sup>, HO<sup>2-</sup> and HO<sup>\*</sup>) that are generated from O<sub>2</sub> reacting with conduction band (CB)

electrons like many other liquid- or gas-phase photocatalytic reactions<sup>[26-28]</sup>. On the other hand, in the present case where TiO<sub>2</sub> particles were buried in the polymer matrix, the surface OH groups were gradually depleted with irradiation. Although the surface OH groups were almost completely depleted after 48 h irradiation, the photocatalytic degradation of PU matrix steadily continued up to 250 h as shown in Figure 7. The C–H bands cleaved in the PU/TiO<sub>2</sub> composite film under irradiation in solid-phase due to higher photocatalytic activity of TiO<sub>2</sub> particles buried in the polymer matrix but remained intact in the pure PU film under irradiation. However, the initiation in the photocatalytic decomposition of PU is quite different. The photodecomposition initiates indirectly through oxidative radicals generated on TiO<sub>2</sub>. The degradation process spatially extends into the PU matrix through the diffusion of the active oxygen species. Once the carbon-centered radicals are introduced in the PU chain, their successive reactions lead to the chain cleavage with the oxygen incorporation and CO<sub>2</sub> evolution.

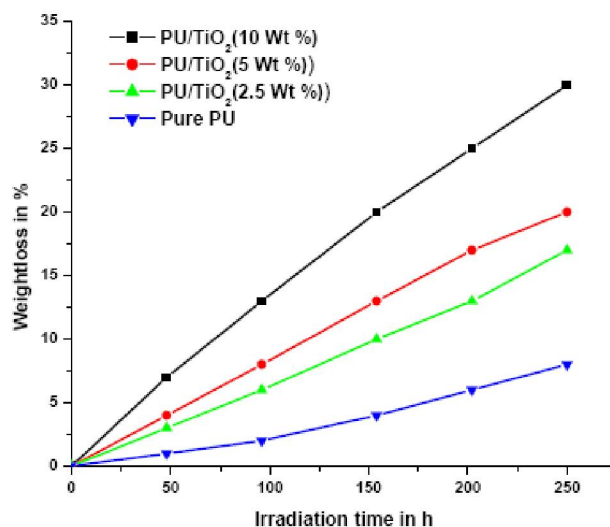


Figure 7 : Weight losses of the pure PU and PU/ TiO<sub>2</sub> composites films during UV light irradiation under aqueous medium

## CONCLUSIONS

The improvement in tensile strength, tensile modulus and dimensional stability, density and % elongation at break of PU/TiO<sub>2</sub> composites was noticed with an increase in the TiO<sub>2</sub> filler content. This can be attributed to the fact that TiO<sub>2</sub> is acting as reinforcing filler in PU matrix. The data obtained from X-ray and FTIR showed

## Full Paper

the physical interaction or interfacial adhesion between the PU and TiO<sub>2</sub> filler. The FTIR and X-ray data supports the improvement in the mechanical performance of the PU/TiO<sub>2</sub> composites. SEM photomicrographs revealed that uniform distribution of TiO<sub>2</sub> filler in PU and the domain size of the second phase depend on the filler content. The merit of using TiO<sub>2</sub> as filler lies in the fact that there is a good physical interaction between the PU and TiO<sub>2</sub> which seems to exhibit good photocatalytic behavior. This study reveals that the photocatalytic decomposition is distinguished from the direct photolytic decomposition of PU in several aspects. Firstly, the photocatalytic decomposition localized on the TiO<sub>2</sub>-PU interface and grew cavities around particles while the direct photolytic centers were uniformly distributed in the PU matrix. Secondly, although both the photocatalytic and photolytic decomposition induced the chain cleavage and the oxygen functionality incorporation, the photocatalytic decomposition was much faster in the weight loss rate. This study demonstrates that the PU/TiO<sub>2</sub> composite has a potential viability to be used as a photodegradable product. On the other hand, the uniform dispersion of TiO<sub>2</sub> particles in the polymer matrix needs to be achieved for commercial applications. This study is successful in this respect and hydrothermally synthesized TiO<sub>2</sub> particles were incorporated into the PU matrix without agglomerates. Using renewable resources like Castrol oil for the preparation of polymer composites is the major scope of the present work.

### REFERENCES

- [1] A.P.Mouritz, A.G.Gibson; 'Fire Properties of Polymer Composite Materials', Springer, (2006).
- [2] T.R.Hull, B.K.Kandola; 'Fire Retardancy of Polymers New Strategies and Mechanisms', RSC, (2009).
- [3] D.Ratna; Epoxy Composites: Impact Resistance and Flame Retardancy Rapra Review Reports, 16(5), (2005).
- [4] K.Friedrich, S.Fakirov, Z.Zhang; 'Polymer Composite from Nano- to Macro-Scale', Springer, (2005).
- [5] G.M.Estes, S.L.Cooper, A.V.Tobolsky; J.Macromol. Sci.Rev.Macromol.Chem., 4, 313 (1970).
- [6] J.W.C.Van Bogart, P.E.Gibson, S.L.Cooper; J.Polym.Sci.Polym.Phys.Ed., 21, 65 (1983).
- [7] J.Ophir, G.L.Wilkes; J.Polym.Sci.Polym.Phys., 18, 1969 (1980).
- [8] Z.Wirpsza; In: T.J.Kemp, (Ed); Polyurethanes: Chemistry, Technology and Applications. Ellis Horwood, New York, (1993).
- [9] J.Blackwell, M.R.Nagarajan, T.B.Hoitnik; Polym., 23, 950 (1982).
- [10] S.P.Pappas, F.H.Winslow; 'Photodegradation and Photostabilization in Coatings', ACS Symposium Series 151, American Chemical Society, Washington, DC, (1981).
- [11] B.Ohtani, S.Adzuma, S.Nishimoto, T.Kagiya; Polym.Degrad.Stab., 35, 53 (1992).
- [12] C.A.Prinet, G.Mur, M.Gay, L.Audouin, J.Verdu; Polym.Degrad.Stab., 61, 211 (1998).
- [13] U.Gesenhues; Polym.Degrad.Stab., 68, 185 (2000).
- [14] H.Behar-Levy, D.Avnir; Adv.Funct.Mater., 15, 1141 (2005).
- [15] H.Behar-Levy, O.Neumann, R.Naaman, D.Avnir; Adv.Funct.Mater., 19, 1207 (2007).
- [16] H.Behar-Levy, D.Avnir; Chem.Mater., 14, 1736 (2002).
- [17] H.Behar-Levy, G.E.Shter, G.S.Grader, D.Avnir; Chem.Mater., 16, 3197 (2004).
- [18] G.E.Shter, H.Behar-Levy, V.Gelman, G.G.Srader, D.Avnir; Adv.Funct.Mater., 7, 913 (2007).
- [19] I.Yosef, D.Avnir; Chem.Mater., 18, 5890 (2006).
- [20] R.E.Dinnebier, S.J.L.Billinge; 'Powder Diffraction Theory and Practice', the Royal Society of Chemistry, Cambridge, UK, (2008).
- [21] Pecharsky, Vitalij, Zavalij, Peter; 'Fundamentals of Powder Diffraction and Structural Characterization of Materials', 2nd Edition, Springer, (2008).
- [22] H.P.Shivaraju; In.J.Environ.Sci., 1(5), 911 (2011).
- [23] H.P.Shivaraju, C.P.Sajan, T.Rungnapa, V.Kumar, C.Ranganathaiah, K.Byrappa; Mater.Res.Innov., 14(1), 80 (2010).
- [24] H.P.Shivaraju, K.Byrappa, S.Ananda; In.J.Chem. Eng.Res., 2(2), 219 (2010).
- [25] C.P.Sajan, B.Shahmoradi, H.P.Shivaraju, K.M.Lokanatha Rai, S.Ananda, M.B.Shayan, T.Thonthai, G.V.Narasimha Rao, K.Byrappa; Mater.Res.Innov., 1(14), 89 (2010).
- [26] D.F.Ollis, H.Al-Ekabi, (Eds); 'Photocatalytic Purification and Treatment of Water and Air', Elsevier, Amsterdam, (1993).
- [27] M.R.Hoffmann, S.T.Martin, W.Choi, D.W.Bahne-mann; Chem.Rev., 95, 69 (1995).
- [28] A.Mills, S.L.Hunte; J.Photochem.Photobiol.A: Chem., 108, 1 (1997).